Some Basic Problems in Flexible-Pavement Design

NORMAN W. MCLEOD, *Engineering Consultant*
Department of Transport, Ottawa, Canada

WITH respect to the stresses applied by wheel loads to airport and highway surfaces, there are three basic problems of flexible pavement design: (1), sufficient thickness of base and surface must be placed over the subgrade to prevent failure within the subgrade; (2) the shearing strengths of the layers of flexible pavement close to the loaded area, i.e., of the base course and bituminous surface, must be high enough that failure along shear surfaces entirely within the base and surface will not occur; and (3) the possibility of failure of any one layer by squeezing out laterally under the applied load must be studied, e.g., a poorly designed bituminous surface may be squeezed out between the tires of traffic and the base course.

During the past 10 or 12 yr. the first of these three problems has been intensively investigated, and various organizations believe they have developed satisfactory solutions, although there is still no universally adopted method. With the advent of tire pressures up to 300 psi. on jet aircraft, and the possibility that these inflation pressures may go higher, answers to the second and third problems have become important. A rational solution to the third problem, insofar as the stability of the bituminous pavement is concerned, has been described in previous papers. It is the principal objective of the present paper to outline a rational approach to the solution of the second major problem—to the problem of avoiding failure along shear surfaces entirely within the base course and bituminous surfacing.

This rational approach is based upon the determination of the c and ϕ values for each layer of the flexible pavement by means of the triaxial test, and upon the assumption that the surfaces of shearing failure are logarithmic spirals. By trial and error, the position of the critical logarithmic spiral is located along which the shearing resistance of the materials will support the smallest ultimate applied load. The wheel load and tire pressure for which the flexible pavement is designed must not exceed this ultimate strength after it has been reduced by a suitable safety factor.

In essence, this method involves the determination of c and ϕ values for an equivalent homogeneous material having the same ultimate strength as the layered system of the flexible pavement. The ultimate strength of this equivalent homogeneous material is calculated on the basis of a logarithmic spiral failure surface.

● FOR many years, one of the principal problems in flexible pavement design for both highways and airports has been the determination of the minimum thickness of granular base and surface required to prevent subgrade failure under any specified wheel load, that is, the emphasis in flexible pavement design has been placed on the avoidance of subgrade failure. The tremendous increases in the wheel loads of aircraft (from about 12,500 lb. for the DC-3 to nearly 200,000 lb. for the B-36), that occurred during and following World War II, focused the attention of both airport and highway engineers on this problem as it never had been before. During the past 10 or 12 yr., large sums have been spent by a number of organizations on research directed toward its solution. While there is still no universally accepted formula for determining the minimum thickness of flexible pavement that must be placed on any given subgrade to support any specified wheel load, various airport and highway agencies appear to feel that they have individual methods that answer this problem at least to their own satisfaction (*1*, *2*, *3*, *4*, *5*, *6*, *7*, *8*). As a result of the marked attention

it has received in recent years, the necessity for this minimum thickness of flexible pavement to prevent subgrade failure is now clearly recognized by highway and airport engineers everywhere.

Since the end of World War II, there has been a vast increase in highway traffic, particularly in the number of heavy axle loadings. In air transport, the introduction and rapid improvement of jet-engine airplanes has been the major development. Reduction in the size of jet aircraft landing gear has been achieved by equipping them with smaller tires inflated to from 200 to 300 psi., and these inflation pressures may go higher. These high tire pressures have brought new problems to flexible-pavement design for airports, because of the high shearing stresses they create in the portion of the pavement close to the loaded area, that is, in the bituminous pavement and the upper portion of the base course. To a lesser degree this is also true of flexible pavements required for the heavy axle loadings and relatively high tire pressures of truck traffic on highways. Consequently, the increased gross loadings and high tire pressures on airports particularly, and to a smaller extent on highways, have made greater thicknesses of flexible pavement necessary, have intensified the shearing stresses in the layers close to the loaded area, and have increased the tendency for failure along shearing surfaces that are located entirely within the base course and bituminous surface (see Fig. 1).

Another serious problem of flexible-pavement design caused by high tire-inflation pressures is the greater squeezing action on each layer, subbase, base course, and bituminous surface. If the applied pressure is high enough, a weak layer may fail by being squeezed out laterally. This type of failure is more likely to occur in a relatively thin layer of material. The most-common example of this type of failure is the squeezing out of a bituminous pavement between tires and base course.

Consequently, each of the following three separate problems or criteria must be considered in flexible pavement design, insofar as resistance to applied loads is concerned:

1. The overall thickness of subbase, base course, and bituminous surface must be adequate to protect the subgrade from failure under the stresses transmitted from the loaded area.

2. The shearing strengths of the materials in layers close to the loaded area must be greater than the shearing stresses caused by high inflation pressures, which tend to cause failure along shear surfaces entirely within the base course and bituminous surface.

3. The stability of each individual layer, subbase, base course, and bituminous surface, must be greater than the tendency of the layer to fail by being squeezed out laterally under the applied load. For example, the bituminous surface must be stable enough to resist being squeezed out between the tire and base course.

As already mentioned, the first of these three

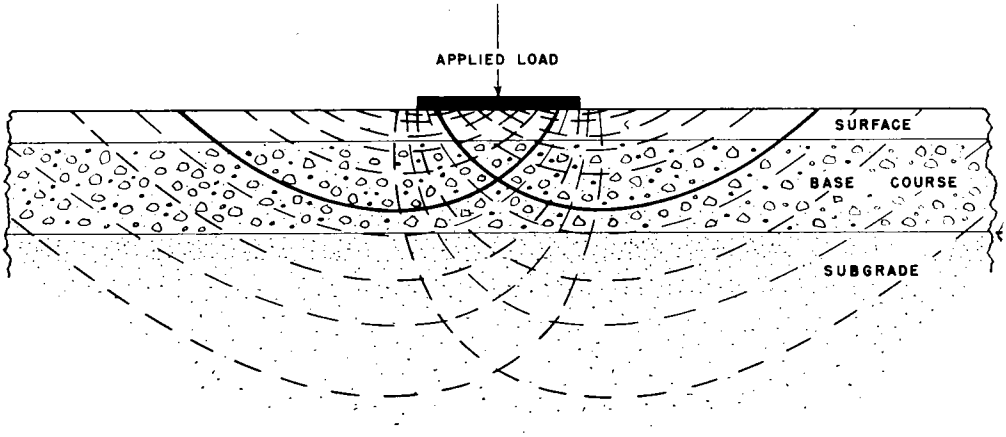

Figure 1. Diagram of shear planes under a loaded area.

problems of flexible pavement design has already received considerable investigation (*1, 2, 3, 4, 5, 6, 7, 8*). The author has described a rational solution to the third problem in previous papers (*9, 10, 11, 12, 13*), insofar as the stability of the bituminous pavement is concerned. It is the principal purpose of the present paper to outline a rational approach to the solution of the second major problem of flexible pavement design, that is, to the problem of avoiding failure along shear surfaces entirely within the base course and bituminous surfacing when the base course is of great depth.

FLEXIBLE PAVEMENTS ARE LAYERED SYSTEMS

As illustrated in Figure 1, the composite cross-section of a flexible pavement, consisting of subgrade, base course, and bituminous surface, constitutes a layered system. Both empirical and rational methods are available for solving the problem of flexible pavement design with which this paper is primarily concerned; namely, avoiding failure along shear surfaces entirely within the base course and bituminous surfacing.

The best-known empirical method in common use is the C. B. R. test employed by the U. S. Corps of Engineers (*7*). By requiring high C. B. R. values for materials in layers close to the loaded area, the Corps of Engineers believes that shearing failure within the base course can be avoided. The principal criticism of any empirical method is that the safety factor actually being employed cannot be determined.

The only rational method of design that has been proposed so far for the layered system represented by a flexible pavement is that of Burmister (*14*). In this method, each layer, subgrade, base course, and bituminous surface, is assumed to consist of perfectly elastic material. Consequently, insofar as its strength is concerned, the most-important characteristic of the material in each layer is its modulus of elasticity. For any measured or given moduli of elasticity for the subgrade, base course, and bituminous surface, and for any specified deflection of the surface of the pavement under the applied load within the elastic range, the required thickness of flexible pavement can be determined. Partly because of its own individual merit, and partly because of its stimulation toward organized rational thought in this field, Burmister's theory represents an outstanding contribution to flexible-pavement design.

For the principal problem under consideration in this paper, which is the avoidance of failure along shear surfaces wholly within the base course and bituminous surfacing, Burmister's method provides a very definite solution. It requires the use of an adequate thickness of base course and bituminous surface, each with a sufficiently high modulus of elasticity that the specified critical deflection at the surface will not be exceeded by the applied load. Consequently, where shearing failure entirely within the base and surface has occurred, Burmister's method indicates that either the critical surface deflection assumed is beyond the elastic range, or that the moduli of elasticity of the base course and surface materials have been less than his theory requires to prevent failure, or both.

The principal criticism of the Burmister theory that is usually made is its assumption that the soils, aggregates, and bituminous mixtures that make up the various layers of a flexible pavement function as perfectly elastic materials. The actual behavior of many of these is far from elastic. Another criticism is that a critical surface deflection must be arbitrarily assumed, since information does not exist to indicate how this deflection should vary with size of contact area, intensity of inflation pressure, thickness of flexible pavement, etc. Furthermore, the moduli of elasticity of many cohesionless base course aggregates and bituminous paving mixtures seem to lie within a similar range. Wherever this occurs, Burmister's method indicates them to be of equivalent strength in flexible-pavement design. Results developed later in the present paper indicate that this may not be true.

It has been frequently observed that when an earth road consisting of a relatively soft homogeneous clay or loam is overloaded by traffic, a rut forms in each wheel path and upheaval of the displaced material occurs on both sides of the lane. It is also a matter of relatively common observation that when a flexible pavement consisting of subgrade, base course, and bituminous surface is overloaded by traffic, similar rutting and upheaval develops. Therefore, in a qualitative way at least, failure of the layered system of a flexible

pavement when overloaded by wheeled traffic seems to follow the general pattern of failure of a homogeneous soil that has been overstressed by traffic. In both of these cases, failure occurs because the applied wheel load exceeds the ultimate strength of the roadway structure. Expressed in another way, failure takes place because the applied shearing stress exceeds the shearing resistance of the loaded material.

These various considerations have led the author to a different rational approach to flexible-pavement design. Burmister's theory is based upon the assumptions of a critical surface deflection and of elastic performance of the materials in the different layers. In the present paper, an attempt will be made to analyze the flexible-pavement problem on the basis of shearing stress versus shearing resistance. Since the ultimate strength of the flexible pavement is employed, which is far beyond any elastic range of loading the structure may have, the method described in this paper is based upon the plastic rather than the elastic behavior of the materials in the various layers of the flexible pavement.

ULTIMATE STRENGTH OF HOMOGENEOUS SOILS

Various investigators have studied the problem of the ultimate bearing capacity of homogeneous soils. Equations for ultimate strength have been proposed by Prandtl (*15*), Terzaghi (*16*), Krey (*17*), Fellenius (*18*), Meyerhof (*19*), and others. It is beyond the scope of this paper to review each of these critically. However, reference will be made to the principles on which several are based, in order to point out the reasons for the selection of the method adopted in this paper.

One of the earliest simple methods proposed for calculating the ultimate strengths of homogeneous soils was the Terzaghi-Hogentogler equation (*20*, *21*). This was based upon the assumption of failure along the straight-line shear planes *ab* and *bc* in Figure 2(a). Failure occurs when the shearing stress exerted on these shear planes by the applied load exceeds the shearing strength. The shearing resistance of the soil along these failure planes is given by the well-known Coulomb equation $s = c + n \tan \phi$. From the nature of this equation, it is apparent that any factor that will increase the normal pressure n on the plane of failure will add to the magnitude of the $n \tan \phi$ term of the Coulomb equation and thereby increase the shearing strength s of the soil.

The Terzaghi-Hogentogler equation overlooks the possibility that the applied load itself may increase the normal pressure n on the failure plane *bc* in Figure 2(a). Investigations by Housel (*22*), and by Davis and Woodward (*23*, *24*), have shown that spreading of the applied load outward with depth below the loaded area may add considerably

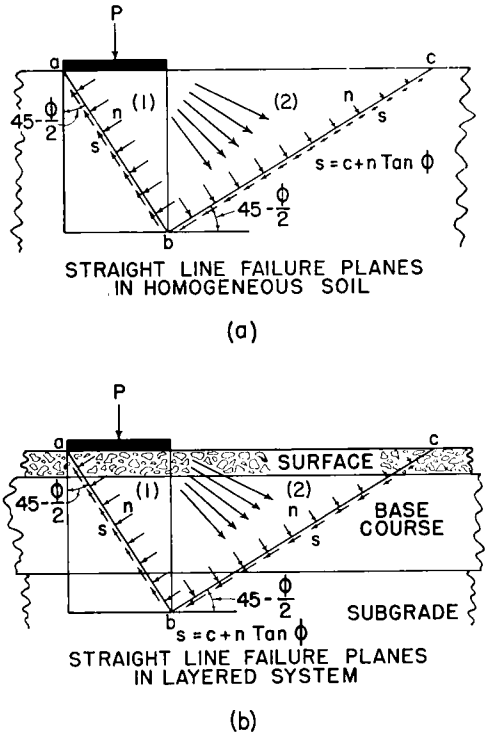

Figure 2. Straight-line failure planes.

to the magnitude of the normal pressure n exerted on the failure plane *bc*. Neglect of this factor makes the Terzaghi-Hogentogler equation for ultimate bearing capacity ultra-conservative.

On the other hand, the manner in which an applied load spreads outward with depth in a homogeneous soil is not known precisely. In the region close to the loaded area at least, this depends upon such factors as the nature of the soil, how the load is applied, e.g., rigid or flexible bearing, etc. As a consequence, the

way in which the normal stress n, due to this spreading of the applied load, varies in magnitude along the failure plane bc is not accurately known and must also be assumed. The calculated ultimate strength in turn will be only as accurate as this assumption. In addition, even after this distribution of normal stress n has been assumed, the summation of the total shearing resistance s, acting along the surface of failure, is not a simple matter, since the $n \tan \phi$ term of the shearing strength varies from point to point along the failure surface.

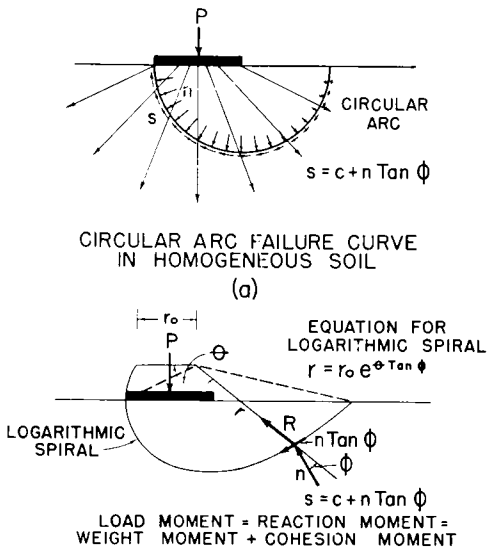

Figure 3. Curved-line failure.

The principal problem, therefore, in obtaining a reasonably accurate ultimate strength value for a homogeneous soil, even on the basis of the simple failure planes in Figure 2(a), is due to uncertainty concerning the magnitude and distribution of the normal stress n acting on the failure plane bc. It should be particularly noted that this introduces equal uncertainty into the value of the $n \tan \phi$ term of the Coulomb equation for the shear strength s of each individual element of length along the failure surface bc.

Recent theoretical studies of the shape of the pressure bulb in a layered system by Fox (*25*) at the National Physical Laboratory (England) have shown that the pattern of pressure distribution on horizontal planes below a loaded surface is still less certain for a layered than for a homogeneous system. Consequently, if it is not easy to determine the ultimate bearing capacity of a homogeneous soil on the basis of the simple straight line failure planes of Figure 2(a), it is still more difficult to do so for the layered system of Figure 2(b). In both cases, accurate values for the shearing resistance s can not be calculated because the magnitude and distribution pattern of the normal pressure n on the plane of failure is not definitely known.

The circular-arc failure curve proposed by Fellenius (*18*) can be used for the determination of the ultimate strength of a homogeneous soil, Figure 3(a). The critical circular arc is found by trial and error and is the arc along which the shearing resistance of the soil will support the lowest ultimate load. The ultimate strength is obtained by equating the moment of applied load about the center of the critical circular arc to the reaction moment about the same point. The reaction moment consists of the summation of the tangential shearing resistance on all elements of the circular arc multiplied by the radius of the arc. Here again, however, the same difficulty that has already been described in connection with Figures 2(a) and 2(b) still arises. The magnitude of the normal pressure n acting on each element of the circular arc is not definitely known. Consequently, the value of the $n \tan \phi$ term of the Coulomb equation for shearing resistance acting tangentially along each element of the circular arc cannot be determined without making assumptions concerning the pattern of lateral distribution of the applied load below the loaded area. The calculated ultimate strength can be no more accurate than these assumptions. In addition, the calculation of the part of the reaction moment due to the $n \tan \phi$ portion of the tangential shearing resistance along the circular arc of Figure 3(a) is a time-consuming task, particularly since the center of the critical circular arc must be found by trial and error. These difficulties do not arise of course, when applying Fellenius' method to homogeneous cohesive soils for which the angle of internal friction $\phi = 0$.

When discussing the determination of the ultimate bearing capacity of a homogeneous

soil by the methods illustrated in Figures 2(a), 2(b), and 3(a), it has been shown that a major difficulty arises because the value of the normal stress n to be used in the Coulomb equation for shearing strength, $s = c + n \tan \phi$, is not accurately known. This problem leads to considering whether there is any alternative approach to the calculation of ultimate bearing capacity, which would eliminate the $n \tan \phi$ term of the Coulomb equation, and substitute for it some other quantity that can be accurately measured or calculated.

As illustrated in Figure 3(b), the assumption of a logarithmic spiral failure curve meets these requirements, provided the ultimate strength is obtained by equating the load moment to the reaction moment. Two symmetrical-spiral failure curves normally occur about a strip load, but in Figure 3(a) the spiral on only one side is shown. Figure 3(b) demonstrates that the resultant of the intergranular normal (n) and frictional ($n \tan \phi$) forces acting at any point along a logarithmic spiral is directed to the origin of the spiral. Consequently, since the moment arm is zero, the moment of the resultant of the intergranular stresses (n and $n \tan \phi$), at any point along the spiral, about the origin of the spiral, is always zero. On the other hand, due to the shape of the logarithmic spiral, there is a greater weight of material within the spiral to the right than to the left of the vertical through the origin. This creates a weight moment about the origin of the spiral.

For the friction moment due to the $n \tan \phi$ term of the Coulomb equation in the case of the circular arc of Figure 3(a) and other failure surfaces, therefore, the logarithmic spiral failure curve of Figure 3(b) substitutes a weight moment. As previously pointed out, the term $n \tan \phi$ is difficult to evaluate precisely. On the other hand, the weight moment of a logarithmic-spiral failure curve can be readily calculated to any desired degree of accuracy.

The significance of each term of the general equation for the logarithmic spiral,

$$r = r_0 e^{\theta \tan \phi}, \qquad (1)$$

is illustrated in Figure 3(b):

r_0 is the initial radius vector;
r is any other radius vector;
θ is the angle between the two radius vectors r_0 and r, and is measured in radians;
e is the base of natural logarithms and is equal to 2.71828; and
ϕ is the angle of internal friction of the material subjected to load.

When calculating the ultimate strength of a homogeneous soil on the assumption of a logarithmic-spiral failure curve, we employ the well-known principle of mechanics that for equilibrium the sum of the moments of the forces about any point must be equal to zero. In this case, it is most convenient to select the origin of the spiral as the point about which the moments are to be taken.

At equilibrium,

load moment = reaction moment = weight moment plus cohesion moment.

The load moment is obtained by multiplying the total load by the moment arm. The reaction moment consists of two quantities, the weight moment and the cohesion moment.

Since more material is contained within the spiral to the right than to the left of the vertical through its origin, this unbalanced weight results in a weight moment. If the material under load possesses any cohesion, its cohesion c acts as a shearing resistance along the entire length of the spiral. The summation of the moments for cohesion c for each element of length of the spiral about the spiral's origin gives the cohesion moment.

E. S. Barber (*26*) has published several tables of basic data that greatly simplify calculations involving the logarithmic spiral. These enable the weight moment and the cohesion moment for the critical spiral, and the ultimate strength, to be determined quite rapidly for loads applied to homogeneous soils with different c and ϕ values.

The principles involved in the determination of the ultimate strength of a homogeneous soil by means of a logarithmic-spiral failure curve are illustrated by a sample calculation in Appendix A, and can be very easily described. By trial and error, the location of the origin of the spiral along which the shearing resistance of the soil will support the smallest ultimate applied load is found. In this trial-and-error method, the load moment is equated to the sum of the weight moment, and the

cohesion moment for each trial spiral selected. This approach is, therefore, somewhat similar to that employed in the circular-arc method for determining the stability of slopes.

The origin of the critical spiral determined by the trial-and-error method lies on a radius vector through an extremity of the loaded area and making a positive angle θ_1 with the horizontal (Fig. A). For cohesionless soils, the origin of this spiral is at the intersection of this radius vector with the vertical marking 75 percent of the distance toward the opposite extremity of the loaded area. For cohesive soils with zero angle of internal friction, the origin of the spiral is at the intersection of the radius vector with the vertical through the opposite extremity of the loaded area. For soils with both c and ϕ values, the origin of the critical spiral lies on the radius vector

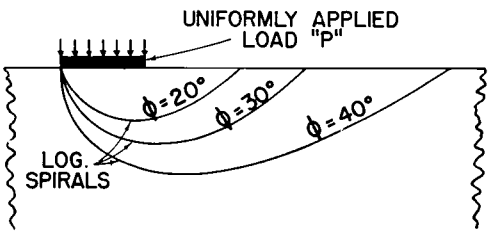

Figure 4. Influence of size of angle of internal friction on the position of the logarithmic spiral-failure curve.

at its intersection with a vertical somewhere between 75 and 100 percent of the distance toward the opposite extremity of the loaded area. The angle $\theta_1 = 23.2$ deg. for the critical spiral for homogeneous cohesive soils for which the angle of internal friction $\phi = 0$, and increases as ϕ is increased. θ_1 approaches ϕ for values of ϕ greater than 45 deg.

To simplify the calculations, unless specifically stated to be otherwise, all data in this paper pertain to the condition of strip loading, that is, for a loaded area which is very long in proportion to its width. The contact area of a loaded tire is elliptical in outline, but the calculations for ultimate strength for this shape of contact area become quite complicated. Other investigators (*27*, *28*) have found that the ultimate unit load supported by a homogeneous cohesive soil on a square or round bearing area is from 20 to 30 percent higher than the ultimate unit pressure supported by the same soil on a strip load of the same width.

To save space in Figures 3(b), 13, and in other diagrams of this paper, only one logarithmic-spiral failure curve, passing through the left extremity of the loaded area and extending toward the right, is shown. In all cases, however, a similar logarithmic-spiral failure curve passing through the right extremity of the loaded area and extending toward the left also exists. The two spirals are symmetrical about the midordinate of the loaded area.

Figure 4 demonstrates how the reaction moment increases with increasing angle of internal friction ϕ of the homogeneous soil being loaded to failure. The length of the logarithmic spiral increases as ϕ increases. This increases both the weight moment and the cohesion moment, which together make up the total reaction moment. Figure 4 also illustrates very clearly how a weight moment is substituted for a friction moment ($n \tan \phi$) in the case of cohesionless soils.

In Figure 5, the increase in the ultimate strength q for a strip load 10 in. wide is illustrated as the angle of internal friction ϕ of a homogeneous cohesionless soil is increased. For highway and airport construction, reasonably well-compacted cohesionless soils would have angles of internal friction normally ranging from about 30 to 50 deg. or slightly higher. On the basis of a logarithmic-spiral failure curve, and the other conditions illustrated in Figure 5(a), it is shown in the graph in Figure 5(b) that as the angle of internal friction ϕ changes from 30 to 50 deg., the ultimate strength q of a cohesionless soil increases from about 16 psi. to about 1,000 psi.

Figure 6 demonstrates the large increase in ultimate strength q that would be possible if the angle of internal friction ϕ of a soil were maintained constant at 35 deg., while its cohesion c was increased from 0 to 14 psi. For the conditions illustrated in Figure 6(a), it is observed from the graph of Figure 6(b) that the ultimate strength q is increased from 37 psi. when $c = 0$, to 342 psi. when $c = 5$ psi., to 883 psi. when $c = 14$ psi. Nijboer (*29*) has reported the results of some triaxial tests on a sand in both the dry and moist states. No difference in the angle of internal friction ϕ occurred between the moist and dry condition in these tests. However, he found that the

cementing or binding effect of the moisture films on the moist sand provided a value for cohesion c = 1.4 psi. Of particular interest, therefore, is the increase in ultimate strength q from 37 psi., when c = 0 and ϕ = 35 deg., to 125 psi., when c = 1.4 psi. and ϕ = 35 deg., shown in Figure 6(b). This is at least qualitatively in keeping with the large variation in the ultimate strength of beach sand between the moist and dry states, that is a matter of common experience.

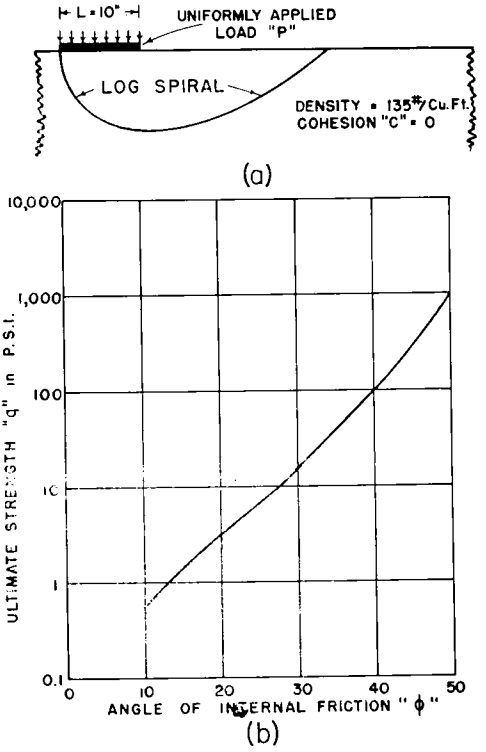

Figure 5. Influence of angle of internal friction on the ultimate strength of a cohesionless soil.

Natural deposits of the good gravel aggregates required for stable base courses are becoming depleted. While large deposits of sands and inferior gravels are still readily available, their stability is too low for service as base course materials, particularly for traffic on tires inflated to high pressures, which tend to cause failure within the base. Figure 6 demonstrates that by the use of a suitable binder the stability of these inferior aggegates could be increased to the extent required for good base-course performance. For example, from a comparison of Figures 5(b) and 6(b), it is seen that if to an inferior aggregate with an angle of internal friction ϕ = 35 deg. a binder can be added to give a cohesion c = 1.0 psi. without decreasing ϕ, its ultimate strength q becomes 100 psi., Figure 6(b), which is the same as the ultimate strength of a cohesionless gravel for which ϕ = 40 deg., Figure 5(b). If to the material for which ϕ = 35 deg., the added binder gives cohesion c = 6 psi. with no reduction in ϕ, its ultimate strength becomes 403 psi., Figure 6(b), which is identical

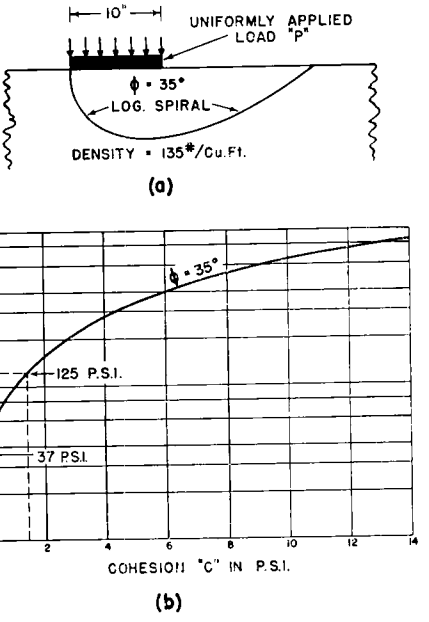

Figure 6. Influence of cohesion on ultimate strength.

with the ultimate strength of a cohesionless gravel for which ϕ = 46° 30′, Figure 5(b). Similarly, for ϕ = 35° and c = 14 psi., Figure 6(b), the ultimate strength q = 883 psi. is the same as that for a cohesionless gravel for which ϕ = 49° 30′, Figure 5(b). Therefore, it is possible by the addition of a suitable binder to a cohesionless sand or gravel of low stability to increase its shearing strength or stability to equal that of a cohesionless aggregate of high stability.

Similarly, by adding a suitable binder to increase the cohesion c of loam soils that already have a low cohesion c and an intermediate angle of internal friction ϕ, their

ultimate strength q, or stability, can be increased to equal that of good cohesionless base course aggregates. Although it is probably not always clearly recognized, this is one of the objectives of the stabilization of both cohesive and cohesionless soils for base-course construction.

When adding binders to cohesionless soils (and even to cohesive soils), it must be kept in mind that many binders can function as lubricants as well as cements. When functioning as lubricants, they tend to reduce the angle of internal friction. The cementing action of many binders increases up to a certain binder content, after which the lubricating effect becomes predominant as more binder is added. When the lubricating effect becomes sufficiently pronounced, the decrease in the angle of internal friction ϕ may be large enough that the ultimate strength q may be lowered materially, even though the cohesion c may still be increasing. Figure 7 shows assumed values for ϕ and c for a cohesionless aggregate with an angle of internal friction ϕ = 40 deg., as a binder is added to it. The curve for ultimate strength q in Figure 7 indicates that q increases to a maximum of 1,060 psi. at a binder content of 4.8 percent, after which it decreases as further binder is added. At a binder content of 10 percent, the ultimate strength q is less than that of cohesionless aggregate by itself. Figure 7 emphasizes the need for careful investigation of the influence of any proposed binder on the ultimate strength or stability of a soil to determine that even small percentages of the binder do not decrease rather than increase the stability or ultimate bearing capacity of the soil.

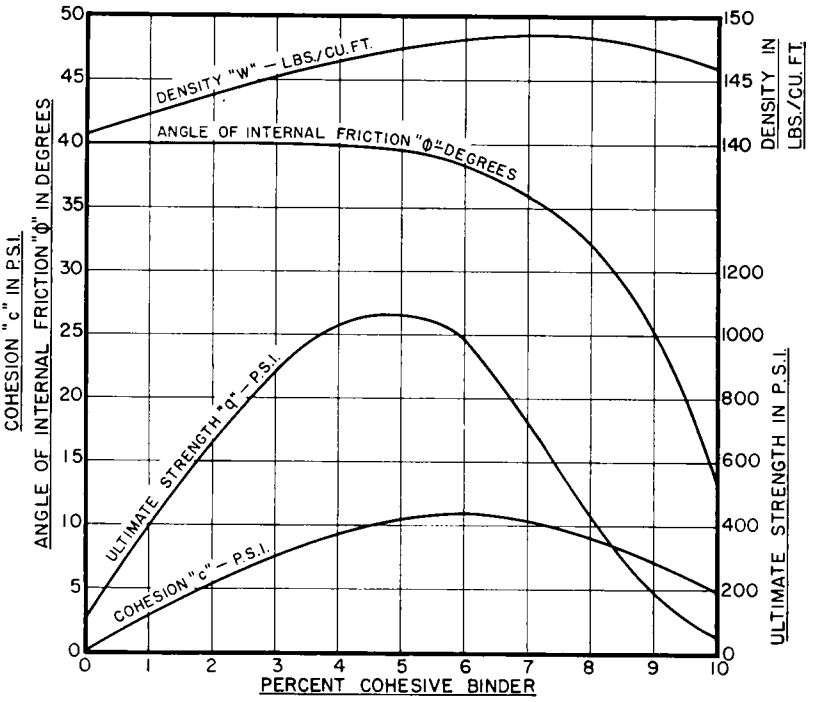

Figure 7. Influence of the addition of a cohesive binder on the ultimate strength of a cohesionless soil.

Figures 6(b) and 7 demonstrate the increase in stability of relatively unstable cohesionless materials that may occur as a cohesive binder is added. They also imply that the stability of even a highly stable cohesionless base course aggregate can be further increased when necessary by the addition of a binder that will give cohesion c without materially decreasing its angle of internal friction ϕ.

Figure 8 illustrates the various combinations of values of c and ϕ for soil materials that are required for a constant ultimate strength q of 200 psi. Figure 8 shows that soils for which c = 36.4 psi. and ϕ = 0, c = 21.5 psi. and ϕ = 10 deg., c = 11 psi. and ϕ = 20 deg., c = 5 psi. and ϕ = 30 deg., c = 1 psi. and ϕ = 40 deg., or c = 0 psi. and ϕ = 44 deg., etc., would all have an ultimate strength of 200 psi. Figure 8, therefore, demonstrates

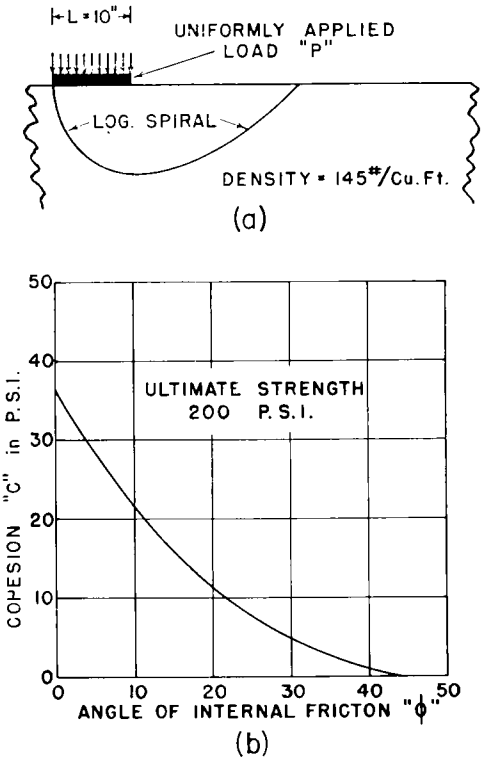

Figure 8. Corresponding values of c and ϕ required to provide an ultimate strength of 200 psi.

further the principle already implied in Figures 6 and 7, that a certain required ultimate strength or stability can be obtained by combining a low angle of internal friction ϕ with a high cohesion c, intermediate values of c and ϕ, or a high angle of internal friction ϕ with a low cohesion c.

Figures 4, 5, 6, 7, and 8 all refer to the ultimate strength of homogeneous soils as determined by means of the logarithmic-spiral approach. It is realized that ultimate-strength values for homogeneous soils can be determined by means of equations for bearing capacity that have been developed by other investigators. For comparative purposes, the ultimate strength values for homogeneous soils given by several of the better known equations for bearing capacity are listed in Table 1.

From the data of Table 1, it is apparent that the logarithmic-spiral provides values for the ultimate strengths of cohesive soils (Columns 2, 3, and 4 in Table 1), that are

TABLE 1
ULTIMATE BEARING CAPACITY OF HOMOGENEOUS SOILS STRIP LOADING

Strip Loading
Width of Loaded Strip = 10 in.
Soil Density = 135 lb. per cu. ft.

Bearing-capacity formula	Ultimate strength values in psi. when			
	c = 5 psi. ϕ = 0	c = 5 psi. ϕ = 20 deg.	c = 5 psi. ϕ = 35 deg.	c = 0 ϕ = 40 deg.
Terzaghi-Hogentogler	20	45	94	8.5
Terzaghi	28.5	92	307	51
Prandtl	25.7	74	117	—
Fellenius	27.6	—	—	—
Logarithmic spiral	27.6	90	338	101

TABLE 2
ULTIMATE BEARING CAPACITY OF COHESIONLESS SOIL STRIP LOADING

Strip Loading
Loaded Strip 1 inch wide; 10 and 24 in. long
c = 0
ϕ = 36 deg.
Density = 102 lb. per cu. ft.

Bearing-capacity formula	Ultimate Strength (psi.)
Actual load test (Davis and Woodward)	14 to 20
Terzaghi-Hogentogler	0.4
Terzaghi	1.5
Logarithmic spiral	3.4

similar to those given by some other bearing capacity equations. For cohesionless soils, on the other hand, the right-hand column in Table 1 shows that the logarithmic spiral gives ultimate strength values which are considerably higher than those derived by other methods.

Davis and Woodward (*23*) report making over 100 bearing-capacity tests on sands. Table 2 contains data taken from their paper, in which they compared the measured ultimate strength of a sand with those calculated by means of several bearing-capacity equations.

In addition, an ultimate strength value calculated on the basis of the logarithmic-spiral method employed for the present paper has been included.

While Table 2 shows that all of the bearing-capacity values calculated by means of the theoretical methods are several times less than that measured by the actual load test on this sand, the ultimate strength calculated by the logarithmic-spiral approach comes closest to the measured value. On this basis, it might be concluded that the logarithmic spiral gives an ultimate strength value for the cohesionless soil (ϕ = 40 deg.) in Table 1, that is only less conservative than those of the other methods. However, in spite of the fact that the logarithmic-spiral method gives best agreement with the measured bearing capacity

TABLE 3

INFLUENCE OF WIDTH OF LOADED AREA AND OF SMALL VALUES OF COHESION c ON THE ULTIMATE STRENGTH OF A COHESIONLESS SOIL WHEN CALCULATED BY THE LOGARITHMIC SPIRAL METHOD

Strip Loading
Width of Loaded Area = L = 1 in. and 10 in.
Density of Sand = 103 lbs. per cubic foot
Angle of Internal Friction ϕ = 36 deg.

	When L = 1.0 in. Cohesion c in psi.			When L = 10 in. Cohesion c in psi.	
	c = 0	c = 0.15	c = 1	c = 0	c = 1
Ultimate strength in psi.....	3.43	14.3	74	34.3	107.8

value in Table 2, it should be mentioned that other investigators have reported good checks between measured values of the ultimate strength of cohesionless soils and those calculated by other bearing-capacity formulas, such as Terzaghi's. It is generally agreed that we still have a great deal to learn about the bearing capacity of soils, and this is emphasized by the variations in the data of Tables 1 and 2.

Table 3 indicates that the large difference between the ultimate strength value measured by Davis and Woodward for a sand understood to be cohesionless, and the values calculated by several theoretical bearing-capacity equations, Table 2, might possibly be due at least in part to the existence of a very small quantity of cohesion c in the sand. For the strip loading width of 1 in., which they used for the data of Table 2, the information in the second and third columns on the left of Table 3 indicates that on the basis of the logarithmic spiral method the calculated ultimate strength would be 3.43 psi. if c = 0, and 14.3 psi. if c = 0.15 psi. Consequently, an actual existence of cohesion c = 0.15 psi. in the sand with which Davis and Woodward were working would account for the entire difference between their measured value of ultimate strength, 14 psi., and the value of 3.43 psi. calculated by the logarithmic-spiral method on the assumption that the sand was entirely cohesionless. A cohesion c = 0.15 psi. is so small that it is within the range of experimental error for most triaxial or direct shear tests and would ordinarily be overlooked or disregarded. It should be recognized that this small value of cohesion c = 0.15 psi. would not necessarily be due to the presence of a binder. Any characteristic of the sand that would lead to the existence of this small intercept on the ordinate axis of the Mohr or Coulomb diagram (the shear strength value at zero normal stress on the plane of failure commonly called cohesion c) would give the large increase in the ultimate strength of the sand that has been listed in Table 3. While this small cohesion c, if it actually existed in the sand used by Davis and Woodward, may have been due to some characteristic other than moisture, it might be mentioned that small quantities of adsorbed moisture can influence the physical properties of sand. This has been pointed out by investigators (*30*) who have endeavored to standardize a given sand for use in the sand method for controlling the compaction of soils in the field. Moisture contents as low as 0.25 percent have been reported to affect the density of a calibrated sand (passing No. 40, retained No. 60 sieve) by as much as 5 lb. per cu. ft. (*30*), when compared with the density of thoroughly dry sand.

Table 3 also demonstrates that the existence of small values of cohesion c in a sand thought to be cohesionless has a much greater influence on ultimate-strength values calculated by the logarithmic-spiral method for very narrow than for wide strip loads. When the width of the loaded strip is only 1 in., a value for cohesion c = 1.0 psi. increases the ultimate strength from 3.43 psi. (for c = 0), to 74 psi., which is 21.6 times as large. On the other hand, for a strip load 10 in. wide, a cohesion c = 1.0 psi. increases the ultimate strength from 34.3

psi. (for $c = 0$), to 107.8 psi., which is only 3.1 times as large. The possibility for unusual results due to unsuspected characteristics of a cohesionless material is, therefore, much greater for very small than for large loaded areas.

It is instructive that Davis and Woodward (*23*) report that the shape of the failure surface observed in their bearing-capacity tests is a logarithmic spiral.

ULTIMATE STRENGTH OF BASE AND SURFACE COURSES

So far, the logarithmic-spiral method has been applied to the determination of the ultimate strength of homogeneous soils. An attempt will now be made to apply this method to the determination of the ultimate bearing capacity of a layered system, such as a flexible pavement. In this section, attention will be concentrated on the ultimate strength of the two-layer system of a bituminous surface resting on a great thickness of granular base. This provides the condition where failure occurs along shear surfaces located entirely within the base and surface course.

Figure 9 considers the case of a bituminous pavement 2 in. thick for which $c = 10$ psi. and $\phi = 40$ deg., resting on a great depth of base of cohesionless material. The ultimate strength of the combined base and surface are to be investigated as the angle of internal friction of the base course is varied from 30 deg. to 40, 50, and 60 deg.

The principal problem in connection with Figure 9, insofar as this paper is concerned, is how the logarithmic-spiral failure curve is to be located through the two layers (surface and base), each with quite different c and ϕ values. The approach to this problem employed in this paper is illustrated in Appendix B, but in essence it involves the determination of c and ϕ values for an equivalent homogeneous material having the same ultimate strength as the layered system of the flexible pavement. The ultimate strength of this equivalent homogeneous material can then be calculated on the basis of a logarithmic-spiral failure surface, as described earlier in the paper; and illustrated in Appendix A. The entire procedure requires a trial-and-error approach involving the use of successive approximations, and consists of the following steps, which by way of example, are based upon the conditions of Figure 9(a) and $\phi = 30$ deg. for the base:

1. As the first step, c and ϕ values must be assumed for the equivalent homogeneous material that is to have the same ultimate strength as the layered system of Figure 9. With more experience, it may be possible to assume a set of c and ϕ values in this first step that are not greatly different from the ultimate values determined at the end of the successive-approximation procedure. This may shorten the number of trials required. As indicated by

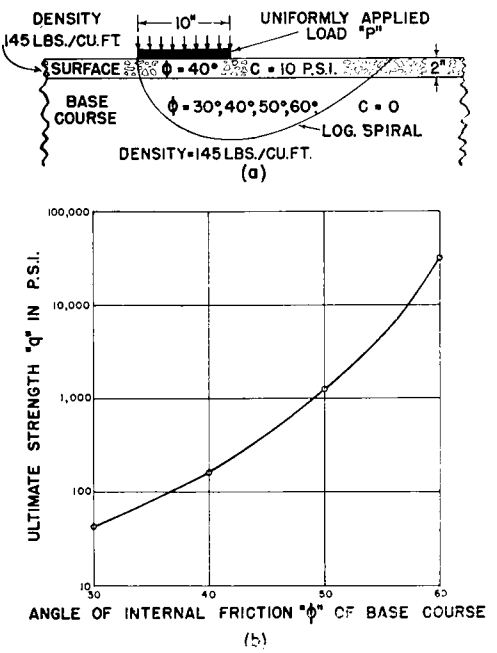

Figure 9. Influence of size of angle of internal friction on the ultimate strength of a flexible pavement.

the set of sample calculations for this particular example in Appendix B, however, the c and ϕ values selected for the first trial were those of the bituminous surface itself ($c = 10$ psi., $\phi = 40$ deg.), although it was obvious that this would lead to a critical logarithmic spiral for which the ultimate strength value would be much too high. For the first trial, therefore, the c and ϕ values assumed for the hypothetical homogeneous material that is to be equivalent in strength to the two-layer system of Figure 9(a) were $c = 10$ psi. and $\phi = 40$ deg.

2. Determine the critical logarithmic spiral for a homogeneous material for which $c = 10$ psi. and $\phi = 40$ deg., by the method outlined in an earlier part of this paper, and illustrated in Appendix A. Calculate the ultimate strength q for this material, which is found to be 1,141 psi. (see Appendix B).

3. Calculate the complete length of this spiral within the base and surface, and also the exact length of each of the two portions of the spiral that lie entirely within the surface course.

4. Using the length of the spiral within the surface course where $\phi = 40$ deg., and the length of the spiral within the base course where $\phi = 30$ deg., calculate an overall arithmetic average value for ϕ for the entire length of the spiral within the base and surface. This gives a value for $\phi = 30$ deg. 26 min. (see Appendix B).

5. Find an overall average value for cohesion c for the entire length of spiral within the base and surface, on the basis that $c = 10$ psi. for the surface course, but is zero for the base course. This can be done in either of two ways. First, by spreading the cohesion $c = 10$ psi. for the part of the spiral within the bituminous surface over the entire length of the spiral as an arithmetic average; that is, the part of the length of the spiral entirely within the bituminous surface multiplied by cohesion $c = 10$ psi., must be equal to the total length of the spiral within the base and surface multiplied by this overall average value for c. Second, by equating the sum of the cohesion moments for the two parts of the spiral entirely within the surface course, to the cohesion moment for the entire spiral within base and surface resulting from the use of an overall average value for cohesion c. The limited number of calculations made to date indicate that a lower value for cohesion c may always result from the use of the first method. It might be generally favored therefore, since a lower value for c results in a more conservative value for ultimate strength. For the present paper, the data for the various diagrams have been calculated partly by one method, and in part by the other. On the basis of the first method, the overall average value of cohesion c for the first trial spiral is $c = 0.437$ psi. (see Appendix B).

6. For the second trial (approximation) determine the critical logarithmic spiral for a homogeneous material for which $c = 0.437$ psi. and $\phi = 30$ deg. 26 min. Calculate the ultimate strength q for this material, which is found to be 34.0 psi.

7. Repeat Steps 3, 4, and 5, on the basis of this second logarithmic spiral and obtain average values for c and ϕ to be used for the third approximation. The new average values found for c and ϕ are $c = 0.739$ psi. and $\phi = 30$ deg. 44 min. (see Appendix B).

8. For the third trial (approximation), determine the critical logarithmic spiral for a homogeneous material for which $c = 0.739$ psi. and $\phi = 30$ deg. 44 min. (see Appendix B). For this spiral the calculated ultimate strength $q = 45.7$ psi.

TABLE 4
VALUES OF c, ϕ, AND q FOR SUCCESSIVE TRIALS
Strip Loading
Width of Loaded Strip = L = 10 in.

Successive Approximation No.	Cohesion c psi.	Angle of Internal Friction ϕ	Ultimate Strength q psi.
1	10	40°	1,141
2	0.437	30°26′	34.0
3	0.739	30°44′	45.7
4	0.660	30°40′	42.6
5	0.675	30°41′	43.2

9. Repeat for as many trials as are necessary to reduce the difference between the ultimate strength values for two successive approximations to an acceptable percentage.

Table 4 summarizes the c, ϕ, and ultimate strength q values for each of the five logarithmic spirals resulting from these successive approximations. It will be observed that the ultimate-strength values for succeeding approximations are alternately on one side of the final value that would result from many successive approximations, and then on the other, Figure C, with the differences between successive approximations gradually becoming smaller. The difference in ultimate strength q between the fourth and fifth successive approximations is only 1.4 percent. Consequently, in this case the fifth successive approximation provides a value for ultimate strength q that would usually be sufficiently accurate for practical design.

On the basis of this logarithmic spiral approach, therefore, the ultimate strength of the layered system of Figure 9(a) in which a

2-in. bituminous surface, for which c = 10 psi. and ϕ = 40 deg., is placed on a great depth of cohesionless base course for which ϕ = 30 deg., is considered to be equal to the ultimate strength, q = 43.2 psi., of a homogeneous material for which c = 0.675 psi. and ϕ = 30 deg. 41 min. (fifth successive approximation in Table 4).

The ultimate strength value, q = 43.2 psi., for successive approximation No. 5 in Table 4 for a layered system consisting of a 2-in. bituminous surface for which c = 10 psi. and ϕ = 40 deg. on a great depth of cohesionless base for which ϕ = 30 deg. has been plotted as the extreme left hand point on the graph in Figure 9(b). This graph indicates that the ultimate strength of the layered system illustrated in Figure 9(a) increases rapidly as the angle of internal friction ϕ of the base course is increased from 30 deg. to 40 to 50 deg. The layered system of Figure 9(a), for which the angle of internal friction ϕ of the base course is 60 deg., is probably of little more than academic interest insofar as normal aggregates are concerned, since its ultimate strength, q = 30,000 psi., is far above the crushing strength of the grains and could not be attained in practice.

Figure 9 emphasizes the increase in resistance to failure along shear surfaces entirely within the base and bituminous surfacing that results from increasing the angle of internal friction ϕ of a great depth of cohesionless base course material beneath a given bituminous surface.

It is instructive to compare Figure 9 with Figure 5 since both pertain to systems in which the angle of internal friction ϕ of a great depth of cohesionless base course material is varied. Figure 9 differs from Figure 5 only in that a 2-in. bituminous surface, for which c = 10 psi. and ϕ = 40 deg. has been substituted in Figure 9 for the top 2 in. of the base course in Figure 5. For ϕ = 50 deg. in the base course, the bituminous surface in Figure 9 has the effect of decreasing ϕ from 50 deg. to 40 deg. in the top 2 in. of Figure 5, but at the same time introduces cohesion c = 10 psi. into this layer. Nevertheless, Figures 5(b) and 9(b) show that when the base course has an angle of internal friction ϕ = 50 deg., the single-layer system of Figure 5 and the two-layer system of Figure 9 both have an ultimate strength of about 1,000 psi. Consequently, introducing a cohesion c = 10 psi. into the top 2 in. of Figure 9(a) just balances the effect of decreasing ϕ from 50 deg. to 40 deg. in this layer, insofar as ultimate strength is concerned. When the base course has an angle of internal friction ϕ = 40 deg. in both cases, the ultimate strength of the single layer system of Figure 5 is 105 psi., while that of the two-layer system of Figure 9 is 160 psi., an increase of about 52 percent. In this case, since the angle of internal friction ϕ is the same for both systems, the increase in ultimate strength is due entirely to the cohesion c of the 2-in. bituminous surface of Figure 9. For the case where the base course has an angle of internal friction ϕ = 30

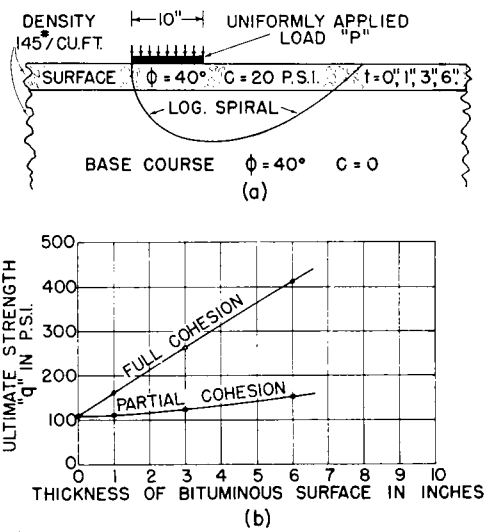

Figure 10. Influence of bituminous-pavement thickness on the ultimate strength of a flexible pavement.

deg., the ultimate strength increases from 16 psi. in Figure 5 to 42 psi. in Figure 9, an increase of about 160 percent. This increase is due partly to increasing ϕ from 30 deg. to 40 deg. in the top 2 in., and partly to the introduction of cohesion c = 10 psi. into this 2-in. layer. The small difference in density, 135 lb. per cu. ft. for Figure 5, and 145 lb. per cu. ft. for Figure 9, does not appreciably affect the comparison that has been made. This comparison between Figure 5 and Figure 9 illustrates the important effect that the introduction of cohesion c into even a part of a layered system has on its ultimate strength.

Figure 10 illustrates the increase in ultimate strength of a layered system consisting of a

bituminous surface on a great thickness of a given cohesionless base course for which $\phi = 40$ deg., as the thickness of bituminous surface is increased from 0 to 6 in. Two graphs are shown. The upper graph, labelled "Full Cohesion," assumes full development of the cohesion of the bituminous surface at both ends of the logarithmic spiral. The graph labelled "Partial Cohesion" is based on the possibility that the structure might have failed before any of the cohesion of the bituminous surface along the right hand side of the spiral has been mobilized. In this latter case, it is assumed that only the cohesion of the bituminous surface traversed by the left-hand side of the spiral of Figure 10(a) is fully developed; that is, the portion of the spiral just under the left-hand extremity of the loaded area.

Figure 10(b) indicates that if the cohesion of the bituminous surface is fully mobilized where it is traversed by both ends of the spiral, the ultimate strength of the layered system of Figure 10(a) increases from 105 psi. for 0 in. of bituminous surface, to 260 psi. for 3 in., to 410 psi. for 6 in. of bituminous surface.

On the other hand, if the cohesion of the bituminous pavement is developed only where it is cut by the left-hand side of the logarithmic spiral, the graph of Figure 10(b) labelled "Partial Cohesion" shows that the ultimate strength of this layered system increases from 105 psi. for zero thickness of bituminous surface, to 120 psi. for a thickness of 3 in., to 160 psi. for a 6-in. thickness of bituminous surface.

Experimental data are required to determine which of the curves of Figure 10(b), or whether some other relationship, applies in actual practice. Nevertheless, when the base itself is not highly stable, Figure 10 indicates that a greater thickness of well-designed and well-constructed bituminous surface of good stability may increase the overall resistance of the base and surface to shearing failure under high tire pressures.

It should be particularly noted in Figure 10 that the angle of internal friction for both the base and surface course is exactly the same, $\phi = 40$ deg. Consequently, the increase in ultimate strength of the layered system of Figure 10 with increase in thickness of the bituminous surface, again reflects the importance of introducing cohesion c into even one part of the layered system.

It should be emphasized that the ultimate strength values that have been given in this section pertain only to resistance to failure along shear surfaces that lie entirely within the base and surface.

SQUEEZING FAILURE OF BITUMINOUS SURFACE BETWEEN TIRE AND BASE

Figure 11 demonstrates the possibility of another type of flexible pavement failure that must always be investigated, particularly where high tire inflation pressures are involved.

Figure 11(a) shows that a great thickness of cohesionless aggregate, for which $\phi = 47$ deg. and $c = 0$, has an ultimate strength of 467 psi. Figure 11(b) indicates an ultimate strength of 254 psi. for a great thickness of bituminous surfacing material for which $c = 10$ psi. and $\phi = 25$ deg. Combining these materials in the two-layered flexible pavement structure illustrated in Figure 11(c) results in an ultimate strength of 465 psi., when the ultimate strength is calculated by means of the logarithmic-spiral method.

However, Figure 11(d) demonstrates the effect of investigating the stability of the layered system of Figure 11(c) on an entirely different basis. The possibility of failure of the bituminous surface by squeezing out between the tire and base course is examined by a method described in detail elsewhere (*9*, *10*, *11*, *12*, *13*). The results of this investigation are illustrated in Figure 11(d). For the shape of the tire-pressure-distribution curve and other conditions shown in Figure 11(d), these results indicate that under any tire inflation pressure greater than about 100 psi. this particular bituminous surface ($c = 10$ psi., $\phi = 25$ deg.) would fail by being squeezed out between the tire and the base course, since some portion of the tire-pressure-distribution curve would be above the pavement-stability curve, that is, the applied pressure on some part of the bituminous surface would exceed its stability. Consequently, in this case the ultimate strength of the layered system is not 465 psi. as given by the logarithmic-spiral method, Figure 11(c), but is about 100 psi., Figure 11(d), as given by the investigation of its resistance to being squeezed out between the tire and base course. If the conditions of

design require a higher unit load than 100 psi. to be carried, Figure 11 indicates that a bituminous pavement having a higher stability against failure by squeezing action than that illustrated, (c = 10 psi. and ϕ = 25 deg.), must be selected.

The data shown in Figure 11 demonstrate the necessity for applying the three criteria outlined at the beginning of this paper to every flexible pavement design problem: (1) sufficient thickness to prevent subgrade failure; (2) adequate shear strength in the layers close to the loaded area to avoid failure along shear surfaces entirely within the base and surface; and (3) examination of the stability of each layer against failure by squeezing action. A different ultimate strength for any given flexible pavement will usually be established by each of the three criteria. It is obvious that the lowest overall strength established by any one of these criteria is the ultimate strength value that should control design.

FLEXIBLE-PAVEMENT DESIGN

It is apparent that the logarithmic-spiral method that has just been described provides a possible basis for the rational design of flexible pavements from the point of view of their over-all thickness requirements. This is illustrated in Figure 12, where the logarithmic-spiral failure curve is seen to cut through bituminous surface, base course, and subgrade.

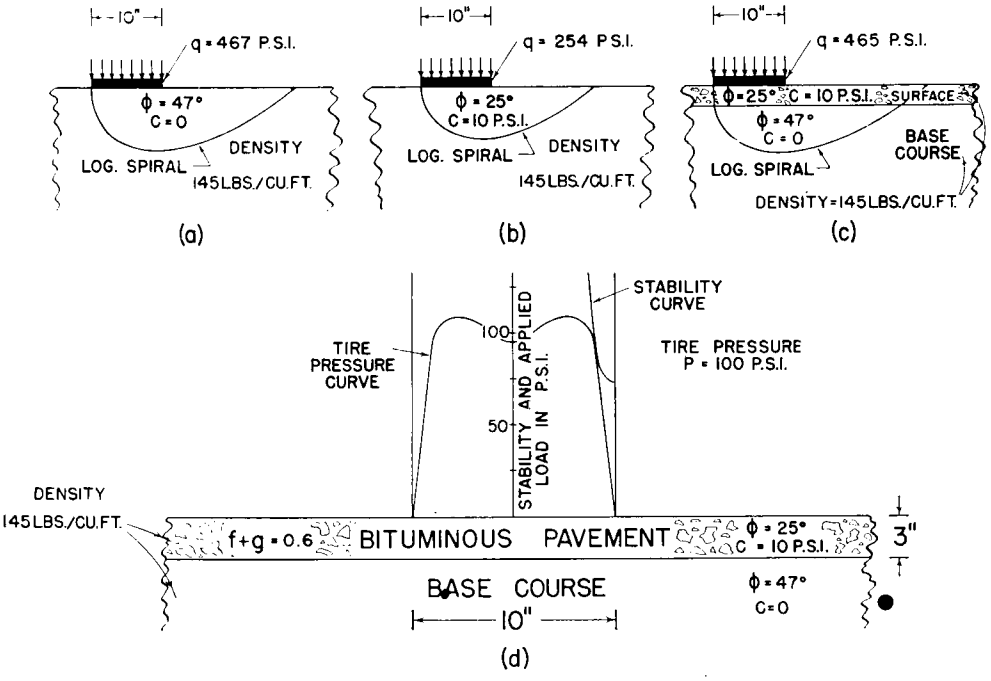

Figure 11. Illustrating failure criteria for flexible pavements.

In this case, the problem consists essentially of determining c and ϕ values for an equivalent homogeneous material that will have the same ultimate strength as that of the three-layer system of Figure 12, comprised of three different materials, each with its own c and ϕ values. On the basis of these over-all c and ϕ values for the equivalent homogeneous material, the critical logarithmic-spiral failure curve can be determined, from which the ultimate strength of the three-layer system is then calculated. The procedure is similar to that already outlined for a two-layer system.

In Table 5, ultimate-strength values are given for a three-layer system of bituminous surface, base course, and subgrade, each having the c and ϕ values and the thicknesses listed. Three strip-loading widths were employed, 10, 12, and 22 in. For each strip-loading width, the only variable is the value of cohesion c of the base course, every other factor being held constant. The data in Column 5 demonstrate that the logarithmic spiral has penetrated well into the subgrade in each case, since its maximum depth of penetration, Z, considerably exceeds the combined thicknesses of surface and base. Other investigators have indicated that the ultimate strength for a circular bearing area is from 20 to 30 percent larger than for a strip load of the same width (*27*, *28*). Since it is usual to base airport and highway pavement design on circular contact areas, frequently considered to be equal to the wheel load divided by the tire inflation pressure, ultimate-strength values for circular bearing areas are shown in the right-hand column of Table 5, and were obtained by increasing the ultimate strengths for strip loading by 25 percent.

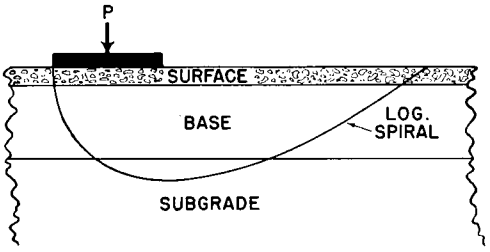

Figure 12. Flexible pavement thickness design.

TABLE 5
ULTIMATE STRENGTH OF FLEXIBLE PAVEMENT
Surface Course c = 10 p.s.i., ϕ = 40 deg.
Base Course c = Variable ϕ = 45
Subgrade c = 8 p.s.i., ϕ = 10 deg.
Strip Loading

Width of Loaded Strip	Thickness of Bituminous Surface	Thickness of Base Course	Total Thickness Base and Surface	Depth of Penetration of Logarithmic Spiral Below Surface	Ultimate Strength	
					Strip Loading	Circular Bearing Area
in.	*in.*	*in.*	*in.*	*in.*	*psi.*	*psi.*
When c = 0 for Base Course						
10	2	6	8	13	134	167
12	3	11	14	18.5	173	216
22	3	17	20	29.5	145	182
When c = 1 psi. for Base Course						
10	2	6	8	13.2	141	176
12	3	11	14	18.4	184	230
22	3	17	20	29.6	152	190
When c = 5 psi. for Base Course						
10	2	6	8	13.2	167	209
12	3	11	14	18.3	235	294
22	3	17	20	29.6	183	229

The data of Table 5 demonstrate that for the otherwise-constant conditions listed for each of the three loaded widths, the ultimate strength of the flexible pavement structure increases as the cohesion c value of the base course is increased from 0 to 1 to 5 psi. The effect on the ultimate strength is small when the cohesion c of the base course is changed from 0 to 1 psi., but the ultimate strength is increased by from 25 to 35 percent when the cohesion c of the base is increased from 0 to 5 psi. (for the cases covered by Table 5).

Consequently, on the basis of the logarithmic-spiral method described in this paper, the data of Figure 5 emphasize again that increasing the cohesion c of any one layer of the flexible-pavement structure within the logarithmic spiral, without sacrificing angle of internal friction ϕ, results in an over-all increase in the ultimate strength of the structure.

SAFETY FACTOR FOR ULTIMATE-STRENGTH VALUES FOR FLEXIBLE-PAVEMENT DESIGN

The ultimate-strength values derived on the basis of the logarithmic-spiral method described in this paper could not ordinarily be employed directly for flexible-pavement design, because the deflection developed by the load at ultimate strength would usually damage the bituminous surface. This is similar to the situation in foundation design where, if the ultimate strength of the underlying soil were employed for the design of footings, the large ensuing settlement would normally damage the structure seriously. When designing footings, a safety factor of about 3 is frequently applied to the measured ultimate strength of the soil (*27*).

Consequently, a factor of safety must usually be applied to the ultimate strength of a flexible pavement as calculated by the

logarithmic-spiral method, to protect the bituminous surface against damage by the excessive deflection that an applied wheel load equal to the ultimate strength would cause. This immediately leads to the problem of what the magnitude of this safety factor should be.

Factors of safety in actual use for flexible-pavement design and construction for highways and airports are unknown. Nevertheless, they could be determined. Actual experience in many areas has indicated what the flexible-pavement design should be for any given wheel load, subgrade support, and traffic intensity. For design purposes, the size of the contact area is usually taken to be equal to the wheel load divided by the tire-inflation pressure and is assumed to be circular in shape. By using the diameter of this circle as the width of a strip loading, and knowing the c and ϕ values for subgrade, base course, and bituminous surface, and the density of each layer, an ultimate-strength value for the flexible pavement can be determined by the logarithmic-spiral method. The ultimate strength for the strip loading can be increased by from 20 to 30 percent to give the corresponding ultimate strength for a circular area of the same diameter as the strip load width. The ratio of this calculated ultimate strength for the circular area in pounds per square inch, to the tire inflation pressure in pounds per square inch employed for the original design, represents the safety factor being used.

Since the required flexible-pavement thickness for any given wheel load and inflation pressure varies with traffic intensity, the safety factor being employed will also vary with the density of traffic. It is quite likely that the safety factor being employed for flexible pavements for airport runways for capacity operations is somewhat smaller than that for highways for densest traffic, since the concentration of traffic is greater on a heavily travelled highway than on the busiest runway.

GENERAL COMMENTS

1. One of the criticisms of the logarithmic-spiral method described in this paper for determining the ultimate strength of flexible pavements that may be suggested is that no allowance has been made for the discontinuities that may occur where the spiral crosses the boundaries between different layers. This objection may be quite valid. On the other hand, the lack of complete homogeneity of soils in embankments and slopes does not seem to interfere with the reasonable accuracy obtained when circular arcs are assumed for the shape of the failure surfaces when analyzing their stability. In stability investigations, these circular arcs are assumed to cut through soil layers of different shearing strengths without discontinuity. In addition, as pointed out early in the paper, the surface profile of the rutting and upheaval of a flexible pavement that has failed under excessive wheel loads is at least qualitatively similar to that of a homogeneous soil which has been overloaded by traffic. Consequently, the shapes of the surfaces of shear failure cannot be greatly different in these two cases, and in this paper they are assumed to be logarithmic spirals. It may be, therefore, that any actual discontinuities that may occur wherever the logarithmic spiral crosses a boundary between two layers of materials are not too important insofar as stability analysis by the logarithmic-spiral method is concerned.

2. When attempts are made to analyze the stability of a layered system by assuming that discontinuities occur wherever the logarithmic-spiral crosses a boundary between two layers, serious difficulties immediately arise. For example a different origin must be located for the portion of the spiral in each layer. The position of each origin will depend upon the amount of discontinuity assumed. In addition, about which of these origins or other common point is the load moment to be taken? Consequently, if discontinuities of the spiral at boundaries between layers are assumed, other assumptions must eventually be made that may lead to greater error than occurs by disregarding them, as has been done in the present paper.

3. When analyzing the stability of slopes by means of the circular-arc method, the shearing resistance of the soil is assumed to be mobilized simultaneously along the whole length of the failure arc, which may be several hundred feet. Good agreement between actual field performance and the stability values calculated on this basis are usually reported. Consequently, the assumption made in this paper that the shearing resistances of the materials in the different layers of a flexible pavement are mobilized simultaneously

throughout the length of a logarithmic-spiral failure curve, which is at most only a few feet in length, may not be unreasonable.

4. One of the major conclusions indicated by the data of this paper is the important influence of cohesion c on the resistance of a flexible pavement to failure along shear surfaces that lie entirely within the base and surface, and probably on failure surfaces that penetrate the subgrade as well. Figures 9 and 10 testify to its importance even when cohesion c is confined to the bituminous surface that has been laid on a base of cohesionless aggregate. The marked effect of cohesion c on the stability of base course material is demonstrated by Figures 6 and 7.

The binders that provide cohesion c may function as lubricants as well as cements. In their capacity as lubricants they tend to reduce the angle of internal friction ϕ of the aggregate. In some situations, therefore, the introduction of the binder leads to a net loss in stability, because the influence of the reduction in ϕ more than offsets the effect of the increase in c.

In cases where the lubricant property of current common binders, such as clay or bituminous materials, is too pronounced, methods for reducing their lubricant quality and increasing their effectiveness as plastic cements (higher cohesion c) should be considered. As an alternative, new inexpensive binders, that will perform more nearly as desired, might be investigated.

5. Since Burmister's layered-system theory of flexible-pavement design is based upon the elastic properties of the material in each layer, it will result in the same strength rating for either cohesionless materials or those containing a binder to give cohesion c, if their moduli of elasticity are the same. The logarithmic-spiral method employed in this paper, on the other hand, indicates that while two materials, one cohesionless and the other cohesive with both c and ϕ values, might have the same moduli of elasticity, the cohesive material may develop either a higher or lower ultimate strength, depending upon the relative values for ϕ of the two materials. Therefore, while its modulus of elasticity is the most important characteristic of the material in each layer from the point of view of Burmister's theory, the c and ϕ values are the most important properties of the material in each layer of a flexible pavement when its strength is analyzed by the logarithmic-spiral method. Consequently, for the same layered system of base course and surfacing materials, a different strength rating will probably be given by Burmister's theory based upon elastic properties and a critical surface deflection than by the logarithmic-spiral method based upon ultimate strength and a factor of safety. No data are presently available for determining the magnitude and range of the difference in strength given by the two methods.

6. While the calculations required for the logarithmic-spiral method described here are somewhat time-consuming, they are relatively simple and straightforward and can be quickly mastered by any qualified, interested individual. Considerable time might be saved if charts providing basic data concerning the logarithmic-spiral method were prepared.

SUMMARY

1. Three criteria for flexible pavement design are listed.

2. Heavier airplanes for air transport, and a greater number of trucks with heavy axle loadings on highways, have increased the thickness of flexible pavement required to prevent subgrade failure.

3. The high tire-inflation pressures of jet aircraft have increased the tendency for flexible-pavement failure along shear planes entirely within the base and surface course when the base course is of great depth.

4. A logarithmic-spiral method for determining the stability of layers of flexible pavement close to the loaded area is described.

5. The ultimate strength of a homogeneous soil has been calculated on the basis of its c and ϕ values, and assuming a logarithmic-spiral failure curve.

6. The ultimate strength of homogeneous, cohesionless soil increases as its angle of internal friction is increased. Its ultimate strength is also increased if a binder is added to give cohesion c, provided the lubricating quality of the binder does not seriously reduce the angle of internal friction of the aggregate.

7. The ultimate strength of a two-layer system consisting of a bituminous surface on a great depth of cohesionless base course can be calculated on the basis of the c and ϕ values for each layer, and assuming a logarithmic-spiral failure curve.

8. The ultimate strength of this two-layer system increases with an increase in the angle of internal friction of the base course material, and is also increased by the cohesion c of the surface course.

9. An example of the possibility of flexible-pavement failure due to squeezing out of an unstable bituminous surface between tire and base course is included.

10. The ultimate strength of a three-layer system consisting of subgrade, base course, and bituminous surface, has been briefly investigated on the basis of a logarithmic-spiral failure curve and the c and ϕ values for the material in each layer.

ACKNOWLEDGEMENTS

The material presented in this paper forms part of an extensive investigation of airports in Canada that was begun by the Canadian Department of Transport in 1945. Air Vice-Marshall A. T. Cowley, director of Air Services, has the general administration of this investigation. It comes under the direct administration of Harold J. Connolly, superintendent construction, George W. Smith, assistant superintendent construction, and E. B. Wilkins. In their respective districts, the investigation is carried on with the generous coöperation of District Airway Engineers G. T. Chillcott, J. H. Curzon, F. L. Davis, O. G. Kelly, L. Millidge, and W. G. D. Stratton.

The diagrams were drafted by C. L. Perkins and John Ostrum. For the very able manner in which he carried through the large number of calculations involving the logarithmic-spiral required for this paper, the author wishes to make grateful acknowledgement to C. L. Perkins.

REFERENCES

1. "Thickness of Flexible Pavements," *Current Road Problems No. 8-R*, Highway Research Board (1949).
2. NORMAN W. MCLEOD, "Airport Runway Evaluation in Canada," Highway Research Board *Research Report No. 4 B*, October (1947).
3. NORMAN W. MCLEOD, "Airport Runway Evaluation in Canada—Part 2," Highway Research Board *Research Report No. 4 B*—Supplement, December (1948).
4. NORMAN W. MCLEOD, "A Canadian Investigation of Load Testing Applied to Pavement Design," *Special Technical Publication No. 79*, American Society for Testing Materials, April, 1948.
5. NORMAN W. MCLEOD, "Economical Flexible Pavement Design Developed from Canadian Runway Study," *Engineering News-Record*, April 28, May 12, May 26, and June 9, 1949.
6. E. H. DAVIS, "Pavement Design for Roads and Airfields," Road Research *Technical Paper No. 20*, Road Research Laboratory, London (1951) H. M. Stationery Office.
7. *Engineering Manual*, Corps of Engineers, U. S. Army, Part XII, Chapter 2, July (1951).
8. L. A. PALMER AND JAMES B. THOMPSON, "Pavement Evaluation by Loading Tests at Naval and Marine Corps Air Stations," Highway Research Board PROCEEDINGS, Vol. 27 (1947).
9. NORMAN W. MCLEOD, "The Rational Design of Bituminous Paving Mixtures," Highway Research Board PROCEEDINGS, Vol. 29 (1949).
10. NORMAN W. MCLEOD, "A Rational Approach to the Design of Bituminous Paving Mixtures," The Association of Asphalt Paving Technologists, *Proceedings*, Vol. 19 (1950).
11. NORMAN W. MCLEOD, "Application of Triaxial Testing to the Design of Bituminous Pavements," American Society for Testing Materials, *Special Technical Publication No. 106*, (1951).
12. NORMAN W. MCLEOD, "Influence of Tire Design on Pavement Design and Vehicle Mobility," Highway Research Board, PROCEEDINGS, Vol. 31 (1952).
13. NORMAN W. MCLEOD, "Rational Design of Bituminous Paving Mixtures with Curved Mohr Envelopes," The Association of Asphalt Paving Technologists, *Proceedings*, Vol. 21 (1952).
14. D. M. BURMISTER, "The Theory of Stresses and Displacements in Layered Systems and Applications to the Design of Airport Runways," Highway Research Board, PROCEEDINGS, Vol. 23 (1943).
15. "Soil Mechanics for Road Engineers," Road Research Laboratory, London (1952), H. M. Stationery Office.
16. KARL TERZAGHI, "Theoretical Soil Mechanics," John Wiley and Sons Inc., New York (1943).
17. D. P. KRYNINE, "Soil Mechanics," McGraw-Hill Book Co. Inc., New York (1941).
18. DONALD W. TAYLOR, "Fundamentals of Soil Mechanics," John Wiley and Sons Inc. (1948).

19. G. G. MEYERHOF, "The Ultimate Bearing Capacity of Foundations," *Geotechnique*, Vol. 2, No. 4, December (1951).
20. C. A. HOGENTOGLER, "Engineering Properties of Soil," McGraw-Hill Book Co. Inc., New York (1937).
21. GEORGE B. SOWERS AND GEORGE F. SOWERS, "Introductory Soil Mechanics and Foundations," The MacMillan Co., New York (1951).
22. W. S. HOUSEL, "Internal Stability of Granular Materials," American Society for Testing Materials, *Proceedings*, Vol. 26, Part 2 (1936).
23. HARMER E. DAVIS AND RICHARD J. WOODWARD, "Some Laboratory Studies of Factors Pertaining to the Bearing Capacity of Soils," Highway Research Board, PROCEEDINGS, Vol. 29 (1949).
24. D. P. KRYNINE, Discussion, Highway Research Board, PROCEEDINGS, Vol. 29 (1949).
25. L. FOX, "Computations of Traffic Stresses in a Simple Road Structure," Road Research Technical Paper No. 9, Road Research Laboratory, London (1948), (H. M. Stationery Office).
26. E. S. BARBER, Discussion, Highway Research Board, PROCEEDINGS, Vol. 29, (1949).
27. G. G. MEYERHOF, "The Tilting of a Large Tank on Soft Clay," The South Wales Institute of Engineers, *Proceedings* (1951)
28. KARL TERZAGHI AND RALPH B. PECK, "Soil Mechanics in Engineering Practice," John Wiley and Sons Inc., New York (1948).
29. L. W. NIJBOER, "Plasticity as a Factor in the Design of Dense Bituminous Road Carpets," Elsevier Publishing Co. Inc., New York (1948).
30. W. R. GREATHEAD, "Soil as an Engineering Material at Two Major Airports in South Africa," The South African Institution of Civil Engineers, *Transactions* (April 1951).

APPENDIX A

SAMPLE CALCULATION FOR ULTIMATE STRENGTH OF A HOMOGENEOUS SOIL BY THE LOGARITHMIC SPIRAL METHOD

The objective of this sample calculation is the determination of the maximum applied strip load that the homogeneous soil can support without failure for the conditions illustrated in Figure A, assuming the failure curve to be a logarithmic spiral.

The method requires balancing load moment against reaction moment for the incipient failure (equilibrium) condition. For this purpose, the location of the critical logarithmic spiral that develops the minimum reaction moment for this condition must be found. The origin of this critical spiral is determined by the trial-and-error method. Barber (*26*) has published three tables of basic data concerning the logarithmic spiral that greatly facilitate a number of the calculations that must be made.

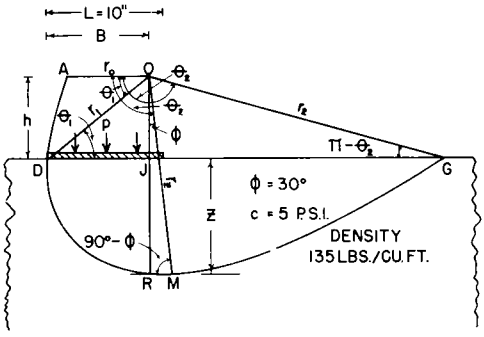

Figure A. Illustrating the logarithmic spiral method for calculating the ultimate strength of a homogeneous soil.

For this sample calculation, the following conditions are given (Fig. A):

Strip Loading
Width of loaded strip = L = 10 in.
ϕ = 30 deg.
c = 5 psi.
Soil Density = w = 135 lb. per cu. ft.

The following information is required: (1) ultimate strength q of the soil in psi. and (2) depth z of the deepest penetration of the critical logarithmic spiral.

As previously shown, the equation for a logarithmic spiral is

$$r = r_0 e^{\theta \tan \phi} \qquad (1)$$

where

r_0 = the initial radius vector
r = any other radius vector
θ = angle between the two radius vectors r_0 and r, measured in radians
e = the base for natural logarithms, 2.71828

ϕ = the angle of internal friction of the material subjected to load

The reaction moment consists of a weight moment plus a cohesion moment. The weight moment is due to the greater weight of material above the spiral to the right than to the left of the ordinate through its origin. The cohesion moment results from the shearing resistance due to cohesion c acting along the length of the spiral. The calculation of the weight moment will be illustrated first.

Step 1

Assume for the first trial that the center of the critical spiral lies on a radius vector through the left extremity of the loaded area making an angle $\theta_1 = 30$ deg., and at a horizontal distance B to the right of the left extremity of the loaded area, Figure A.

Step 2

Calculate values for r_1/r_0, $\sin \theta_1$, r_2/r_0, $\pi - \theta_2$, θ_2, r_0, and r_0^3, all of which are required for determining the weight moment.

By substitution in Equation 1, it is found that $r_1/r_0 = 1.35$, (see also Barber's Table A, which is based on Equation 1, and gives values of r/r_0 for different values of θ and ϕ).

$$\sin \theta_1 = \sin 30^\circ = 0.5$$

To evaluate r_2/r_0, solve the following identity by trial and error.

$$\frac{r_1}{r_0} \sin \theta_1 = \frac{r_2}{r_0} \sin (\pi - \theta_2)$$

from which

$$\frac{r_2}{r_0} = 5.74$$

and

$$\pi - \theta_2 = 6.8^\circ$$

$$\theta_2 = 180^\circ - 6.8^\circ = 173.2^\circ$$

From Figure A by inspection

$$r_0 = \left(\frac{B}{\cos \theta_1}\right)\left(\frac{1}{\frac{r_1}{r_0}}\right) = \left(\frac{B}{\cos 30^\circ}\right)\left(\frac{1}{1.35}\right) = 0.854B$$

$$r_0^3 = 0.623B^3$$

Step 3

Barber (*26*) lists the following equation for the moment of a sector of a logarithmic spiral

$$M = \frac{r_0^3}{3 + 27 \tan^2 \theta} \cdot [e^{3\theta \tan \phi}(\sin \theta + 3 \cos \theta \tan \theta) - 3 \tan \phi] \quad (2)$$

and in his Table C has tabulated values for M/r_0^3 for a wide range of values of θ and ϕ.

The weight moment for the first trial spiral, $\theta_1 = 30$ deg., is calculated as follows:—

Weight moment of spiral sector $OADMGO$ =

$15.75B^3w$ (Barber's Table C (26))

Weight moment of spiral sector $OADO$ =

$0.17B^3w$ (Barber's Table C (26))

Weight moment of triangle $ODJO = (B/2) \cdot (B \tan \theta_1)\ (B/3)\ (w) = 0.096B^3w$

Weight moment of $\triangle\ OJGO = \frac{B \tan \theta_1}{(2)\ (3)} \cdot (B \tan \theta_1 \cot (\pi - \theta_2))^2 w = 2.29B^3w$

Weight moment of section $DMGD$

$$= M_{OADMGO} + M_{OADO} + M_{ODJO} - M_{OJGO}$$

$$= 15.75B^3w + 0.17B^3w + 0.096B^3w - 2.29B^3w$$

$$= 13.73B^3w$$

Therefore, the required value for the weight moment for the first trial spiral = $13.73B^3w$.

Step 4

The cohesion moment for the length of the first trial spiral actually in the soil must now be calculated.

The moment of the length of a section of a logarithmic spiral is equal to twice the area subtended by the section from its origin. Barber (*26*) lists the following equation for the area of a sector of a logarithmic spiral,

$$A = \frac{r_0^2}{4 \tan \theta} (e^{2\theta \tan \phi} - 1) \quad (3)$$

and in his Table B has tabulated values for A/r_0^2 for a wide range of values of θ and ϕ.

TABLE A

CALCULATION OF REACTION MOMENTS FOR DIFFERENT ASSUMED VALUES OF θ_1 FOR A HOMOGENEOUS SOIL FOR WHICH $\phi = 30°$

θ_1	r_1/r_0	$\sin\theta_1$	r_2/r_0	$\pi - \theta_2$	θ_2	r_0	r_0^3	Weight Moments					Cohesion Moment	Total Reaction Moment
								OADMGO	*OADO*	*ODJO*	*OJGO*	Total		
30°	1.35	0.5000	5.74	6.8°	173.2°	$0.854B$	$0.623B^3$	$15.75B^3w$	$0.17B^3w$	$0.10B^3w$	$-2.29B^3w$	$13.73B^3w$	$19.6B^2c$	$B^2(13.73wB + 19.6c)$
35°	1.42	0.5736	5.65	8.3°	171.7°	$0.858B$	$0.635B^3$	$15.02B^3w$	$0.21B^3w$	$0.12B^3w$	$-2.70B^3w$	$12.65B^3w$	$19.0B^2c$	$B^2(12.65wB + 19.0c)$
40°	1.50	0.6428	5.54	10.0°	170.0°	$0.870B$	$0.659B^3$	$14.40B^3w$	$0.27B^3w$	$0.14B^3w$	$-3.14B^3w$	$11.67B^3w$	$18.7B^2c$	$B^2(11.67wB + 18.7c)$
45°	1.57	0.7071	5.45	11.8°	168.2°	$0.900B$	$0.730B^3$	$14.78B^3w$	$0.35B^3w$	$0.17B^3w$	$-3.87B^3w$	$11.43B^3w$	$19.1B^2c$	$B^2(11.43wB + 19.1c)$
50°	1.65	0.7660	5.34	13.8°	166.2°	$0.942B$	$0.839B^3$	$15.49B^3w$	$0.48B^3w$	$0.20B^3w$	$-4.77B^3w$	$11.40B^3w$	$19.7B^2c$	$B^2(11.40wB + 19.7c)$

Consequently,

cohesion moment

= 2c (area of sector of spiral)

= 2c (area $OADMGO$ − area $OADO$)

Area of sector of spiral $OADMGO = 13.78r_0^2$

(Barber's Table B (26))

Area of sector of spiral $OADO = 0.36r_0^2$

(Barber's Table B (26))

from which

cohesion moment = $2c\ (13.78r_0^2 - 0.36r_0^2)$

$= 26.84r_0^2c$

but

$r_0 = 0.854B$ (see Step 2 above)

Therefore, the required value for the cohesion moment for the first trial spiral = $19.6B^2c$.

Step 5

Consequently, for the first trial spiral

Total reaction moment

= weight moment plus cohesion moment

$= 13.73B^3w + 19.6B^2c$

Step 6

Repeat the calculations for Steps 1 to 5 to obtain similar expressions for the total reaction moment when θ_1 is assumed to be 35 deg., 40 deg., 45 deg., and 50 deg. These are summarized in Table 6.

It should be pointed out in connection with Table 6, that the expressions obtained for the reaction moments when assumed values for $\theta_1 = 30$ deg., 35 deg., 40 deg., 45 deg., and 50 deg., will always hold for a homogeneous soil for which $\phi = 30$ deg., regardless of the value of cohesion c. Consequently, the reaction moment expressions listed in Table 6 do not again have to be calculated as long as the angle of internal friction $\theta = 30$ deg. for a homogeneous soil. Similarly, other expressions for reaction moments for assumed values of θ_1 need be calculated only once when $\phi = 40$ deg., and so on.

It will be observed that reaction moment expressions are given for assumed values of θ_1 in 5-deg. intervals in Table A. A limited number of calculations indicate that this results in values for ultimate strength that may be sufficiently accurate for practical design.

Step 7

For this sample calculation it has been assumed that $c = 5$ psi., $\phi = 30$ deg., and $w = 135$ lb. per cu. ft. By substitution of these values for w and c in the reaction moment expressions in Table 6, the minimum reaction moment appears to occur for $\phi_1 = 40$ deg., and is given by the expression $11.67wB^3 + 18.70B^2c$.

It should be noted, however, that each reaction moment expression in Table 6 contains the term B^3 in the weight moment portion, and B^2 in the cohesion moment item. (In Figure A, B is the horizontal distance from the left-hand extremity of the loaded area to the ordinate through the origin of the spiral, and is given by DJ.) The value of B (see Step 10 below) varies somewhat with the values of c, ϕ, and ϕ_1. Consequently, the minimum reaction moment obtained by substituting values for c and w in tables of reaction moments such as Table 6, should be checked by substituting the value for B calculated for reaction moment expressions at and on each side of this apparent minimum to ensure that the minimum reaction moment has been determined.

In this particular case, substitution of the values for w and c gives a minimum reaction moment that is unchanged by the values found for B.

Therefore,

the minimum reaction moment

$= 11.67wB^3 + 18.7B^2c.$

Step 8

From inspection of Figure A, and since $L = 10$, it is apparent that

$$\text{Load moment} = (Lp)\left(B - \frac{L}{2}\right) = 10p(B - 5)$$

Step 9

Equating the load moment to the minimum reaction moment gives

$$10p\ (B - 5) = 11.67wB^3 + 18.70B^2c$$

which upon rearranging becomes

$$p = \frac{11.67wB^3 + 18.70B^2c}{10(B - 5)} \qquad (4)$$

but

w = 135 lb. per cu. ft. = 0.0783 lb. per cu. in.

and

$$c = 5 \text{ psi.}$$

Substitution of these values for w and c in Equation 4 gives

$$p = \frac{0.91B^3 + 93.5B^2}{10(B - 5)} \tag{5}$$

Step 10

In Equation 5, p = unit applied load, while B = the horizontal distance from the left extremity of the loaded area to the ordinate through the origin of the critical logarithmic spiral. It is necessary to find the value for B that will result in the minimum value for p; that is, to find the origin of the spiral that will provide the smallest ultimate strength q. This is obtained by differentiating Equation 5 with respect to p, equating the derivative to zero, and solving the resulting quadratic equation for B.

Differentiating Equation 5, simplifying, and equating the resulting equation to zero, gives

$$\frac{dp}{dB} = B^2 + 43.9B - 513.7 = 0 \tag{6}$$

Solving Equation 6 for B gives

$$B = 9.6 \text{ in.}$$

Consequently, the origin of the required critical logarithmic spiral is located on the radius vector making an angle $\theta_1 = 40$ deg., at the point of intersection of this radius vector with the ordinate spaced 9.6 in. to the right of the left-hand extremity of the loaded strip, Figure A.

Step 11

The ultimate strength q is obtained by substituting the value 9.6 for B in Equation 5, and solving for p, which gives

$$p = 205 \text{ psi.}$$

Therefore, the ultimate strength q for a homogeneous soil for which $c = 5$ psi. and $\phi = 30$ deg., and for the other conditions illustrated in Figure A, is 205 psi.

Step 12

To find the depth z of the deepest penetration of the critical logarithmic spiral below the ground surface.

From Figure A,

Angle $OMR = 90 - \phi$, since the tangent to a logarithmic spiral always makes an angle of $90 - \phi$ with the radius vector at the point of tangency.

Also,

$$\text{Angle } OMR = 180 - \theta_z .$$

Consequently,

$$90 - \phi = 180 - \theta_z$$

or

$$\theta_z = 90 + \phi$$

In addition,

$$z + h = r_z \cos (\theta_z - 90°) = r_z \cos \phi$$

but,

$$h = B \tan \theta_1$$

Therefore,

$$z = r_z \cos \phi - B \tan \theta_1 \tag{7}$$

The value of each term in Equation 7, except r_z, has already been evaluated.

$$\cos \phi = \cos 30° = 0.866$$

$$B = 9.6$$

$$\tan \theta_1 = \tan 40° = 0.8391$$

r_z can be evaluated from the general equation for the logarithmic spiral,

$$r_z = r_0 e^{\theta_z \tan \phi} \tag{8}$$

for which

$$r_0 = 0.870\ B = (0.870)\ (9.6) = 8.35$$

$$\theta_z = 90 + \phi = 90 + 30 = 120° = 2.0944 \text{ radians}$$

$$\tan \phi = \tan 30° = 0.5774$$

Substituting these values in Equation 8 and solving, gives,

$$r_z = 28.0 \text{ in.}$$

All terms on the right hand side of Equation 7 have now been evaluated. Substituting these values in Equation 7 gives

$z = (28.0)\ (0.866) - (9.6)\ (0.8391) = 16.2$ inches

Consequently, the maximum penetration of the critical logarithmic spiral below the ground surface, z, is 16.2 in.

APPENDIX B

SAMPLE CALCULATION FOR THE ULTIMATE STRENGTH OF A TWO-LAYER SYSTEM BY THE LOGARITHMIC SPIRAL METHOD

The objective of this sample calculation is the determination of the maximum applied strip load that a two-layer system consisting of a bituminous surface on a great depth of base course can support without failure for the conditions illustrated in Figure B, assuming the failure curve to be a logarithmic spiral.

In essence, the method employed requires the determination of c and ϕ values for an equivalent homogeneous material having the same ultimate strength as the layered system. After these c and ϕ values have been determined, the ultimate strength of the equivalent homogeneous material can be obtained by the method outlined in Appendix A. It is assumed, of course, that this method is capable of providing c and ϕ values for an equivalent homogeneous material having the same ultimate strength as the layered system.

There is a different material in each layer of the two-layer system of Figure B, and each has its own c and ϕ values. To find the values of c and ϕ for an equivalent homogeneous material having the same ultimate strength as the two-layer system, the method of successive approximations is employed, assuming in all cases that the failure curve is a logarithmic spiral.

As the first step in this method, single values for c and ϕ for the equivalent homogeneous material are assumed, and the critical logarithmic spiral is determined as described in Appendix A. Based on the actual values of c and ϕ for each layer traversed by the spiral, overall average values for c and ϕ assumed to be acting along the full length of the spiral can be calculated. These calculated average values for c and ϕ will usually be different from those arbitrarily assumed for this spiral. A second critical spiral is, therefore, determined, based on a homogeneous material having the average values for c and ϕ calculated for the first spiral. Using the procedure just outlined for the first spiral, overall average values for c and ϕ acting along the full length of the second spiral can be calculated. Using this second set of average values for c and ϕ, a third critical spiral is determined, from which a third set of overall average values for c and ϕ can be calculated, and used for establishing the fourth spiral. This process can be repeated as often as required.

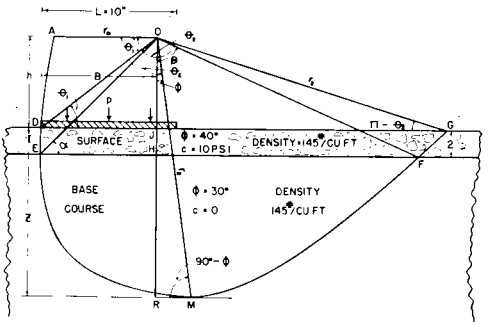

Figure B. Illustrating the logarithmic spiral method for calculating the ultimate strength of a two-layer system of flexible pavement.

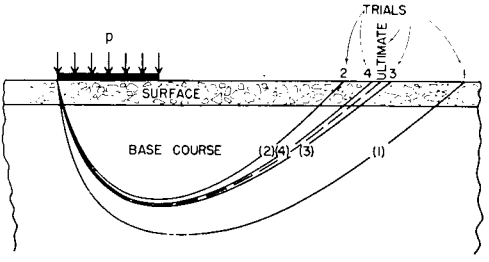

Figure C. Illustrating relative positions of logarithmic spirals resulting from successive trials when applying the method of successive approximations.

As illustrated in Figure C, each successive spiral approaches more nearly to the ultimate spiral that would result from many successive approximations. Table 4 demonstrates that the differences in over-all average values for c and ϕ, and in the values of ultimate strength, become progressively smaller between successive approximations. Consequently, the number of successive approximations to be used in any given case, depends upon the degree of accuracy needed for practical design. For the conditions covered by Table 4, the fifth,

and possibly the fourth, or even the third successive approximation might provide the accuracy required.

The successive steps required for the application of this method will be outlined in a sample calculation based on the following conditions illustrated in Figure B.

Strip Loading

Width of Loaded Strip = L = 10 in.

For surface course, c = 10 psi., ϕ = 40 deg.

For base course, ϕ = 30 deg.

Thickness of surface course = 2 in.

Density of both layers = w = 145 lb. per cu. ft.

= 0.839 lb. per cu. in.

The following information is required: (1) ultimate strength q of the two-layer system in pounds per square inch and (2) depth z of the deepest penetration of the critical logarithmic spiral.

The successive steps required for the determination of the ultimate strength of the two-layer system will be described first.

Step 1

Arbitrarily assume c and ϕ values for the homogeneous material that is to have the same ultimate strength as that of the given two-layer system. With more experience, it may be possible to assume a set of c and ϕ values in this first step that are not greatly different from the ultimate values for c and ϕ determined at the end of the successive approximation procedure, which will be intermediate between those for the surface course and the base course; that is, c should be somewhere between 0 and 4 psi., and ϕ somewhere between 30 deg. and 40 deg. Nevertheless, although they are obviously much too high, the c and ϕ values for the bituminous surface will be selected for the first approximation in this case, since they are rather extreme.

The arbitrarily assumed values for c and ϕ for the equivalent homogenous material for the first step, therefore, are c = 10 psi. and ϕ = 40 deg.

Step 2

Determine the critical spiral for a homogeneous material for which c = 10 psi. and ϕ = 40 deg., by the trial-and-error method outlined in Appendix A. The ultimate strength q for this homogeneous material as calculated from the critical spiral = 1,141 psi. (Table 4).

Step 3

On the basis of the actual values of c and ϕ in each of the two layers traversed by this spiral, determine over-all average values for c and ϕ assumed to be acting along the full length of the spiral. The over-all average value for ϕ will be calculated first.

Step 4

Calculate the total length of this first spiral (below ground level), and also the length of each of the left-hand and right-hand portions of the spiral lying entirely within the surface course.

The length of the arc DMG of the spiral is found by integrating the following equation:

$$\text{Length of arc } DMG = \frac{r_0\sqrt{\tan^2\phi + 1}}{\tan\phi} \cdot [e^{\theta \tan\phi}]_{\theta 1}^{\theta 2} \qquad (9)$$

By the procedure of Step 2, Appendix A,

r_0 = 7.133 in.

θ_1 = 50° = 0.8727 radians

θ_2 = 172° 43′ = 3.0147 radians

$\tan\phi = \tan 40° = 0.8391$

Substituting these values in Equation 9 and simplifying,

Length of arc DMG = 116.16 in.

To find length of arc of spiral DE, angle α must be first evaluated:

B = 9.536 in. (Procedure of Appendix A)

$OJ = B \tan\theta_1$

$\tan\theta_1 = \tan 50° = 1.19175$

$OJ = (9.536)\ (1.19175) = 11.365$ in.

$OH = OJ + 2$ in. = 13.365 in.

$$\frac{OH}{OE} = \sin\alpha$$

Also

$OE = r_0\ e^{\alpha\tan\phi} = 7.133\ e^{0.8391\alpha}$

Then

$$\frac{OH}{\sin \alpha} = 7.133\, e^{0.8391\alpha}$$

or

$$\sin \alpha e^{0.8391\alpha} = 13.365/7.133 = 1.8737 \quad (10)$$

Solving Equation 10 by trial and error gives

$$\alpha = 55°49' = 0.974 \text{ radians}$$

$$\text{Length of arc } DE = \frac{r_0\sqrt{\tan^2 \phi + 1}}{\tan \phi} \cdot [e^{\theta \tan \phi}]_{\theta_1}^{\alpha} \quad (11)$$

Substituting known values for each term on the right-hand side of Equation 11 and simplifying gives

Length of arc DE = 2.052 in.

By a similar series of calculations, it is found that

Length of arc FG = 3.029 in.

Therefore,

Total length of spiral in bituminous surface

= 2.052 + 3.029 = 5.081 in.

Total length of spiral in base course

= 116.16 − 5.08 = 111.08 in.

Step 5

To obtain the overall average value for ϕ along the whole spiral DMG,

$$(116.16)\, \phi_{av} = (5.08)(\phi = 40°) + (111.08)(\phi = 30°)$$

$$\phi_{av} = \frac{(5.08)(40) + (111.08)(30)}{116.16}$$

$$= 30°26'$$

Therefore, the overall average value for ϕ along the length of the first spiral is 30 deg. 26 min.

Step 6

To obtain the overall average value for cohesion c along the whole spiral DMG,

$$(116.16)\, c_{av} = (5.08)(c = 10) + (111.08)(c = 0)$$

$$c_{av} = \frac{(5.08)(10) + (111.08)(0)}{116.16}$$

$$= 0.437 \text{ psi.}$$

Therefore, the overall average value for cohesion c along the length of the first spiral is 0.437 psi.

Step 6 (Alternative)

As an alternative to the method just given in Step 6, an average value for cohesion c can be obtained by equating the sum of the cohesion moments for the two portions of the spiral, DE and FG, entirely within the surface course, to the cohesion moment for the entire spiral, DMG, resulting from the use of this overall average value for cohesion c.

The general equation for the cohesion moment of an arc of a logarithmic spiral is

$$\text{cohesion moment of arc of spiral} = \frac{cr_0^2}{2 \tan \phi} [e^{2\theta \tan \phi} - 1]_{\theta_1}^{\theta_2} \quad (12)$$

From the conditions for this sample calculation, Figure B, cohesion c = 10 psi. for the portion of the spiral within the bituminous surface, and c = 0 for the base. Consequently, cohesion moments for the different parts of the spiral can be calculated.

Cohesion moment for Arc DE

$$= \frac{cr_0^2}{2 \tan \phi} [e^{2\theta \tan \phi} - 1]_{\theta_1}^{\alpha} \quad (13)$$

Substituting known values for each term on the right hand side of Equation 13, and simplifying, gives

Cohesion moment for Arc DE

= 243.6 in.-lb.

Cohesion moment for Arc FG

$$= \frac{cr_0^2}{2 \tan \phi} [e^{2\theta \tan \phi} - 1]_{\frac{\pi}{2} + \beta}^{\theta_2} \quad (14)$$

Substituting known values for each term on the right-hand side of Equation 14, and simplifying, gives

Cohesion moment for Arc FG

= 2046.2 in.-lb.

Cohesion moment for Arc DMG

$$= \frac{c_{av} r_0^2}{2 \tan \phi} [e^{2\theta \tan \phi} - 1]_{\theta_1}^{\theta_2} \quad (15)$$

Substituting known values for each term on the right-hand side of Equation 15, and simplifying, gives,

Cohesion moment for arc $DMG = 4643.5\ c_{av}$ in.-lb.

Equating these cohesion moments,

$$4643.5\ c_{av} = 243.6 + 2046.2 = 2289.8$$

from which,

$$c_{av} = \frac{2289.8}{4643.5} = 0.493 \text{ psi.}$$

Consequently, the overall average value for cohesion c along the length of this first spiral, as obtained by the moment method, is 0.493 psi.

Step 7

Since the over-all average value for cohesion c obtained as an arithmetic average is somewhat smaller than that given by the moment method, it is used here because it is more conservative.

Average values for c and ϕ given by the first spiral (first approximation), which are to be used for the spiral representing the second approximation, therefore, are

$$c = 0.437 \text{ psi.}$$

$$\phi = 30° 26'$$

It will be observed that these average values for c and ϕ calculated for the first spiral are considerably different from the values of c = 10 psi. and ϕ = 40 deg. that were arbitrarily assumed for its construction.

The method of successive approximations must, therefore, be continued until the overall average values for c and ϕ calculated for any spiral are very nearly the same as the values of c and ϕ used for its determination. Expressed in another way, this method must be continued until the over-all average values for c and ϕ calculated for spirals representing two successive approximations, are quite close to each other (Table 4 and Figure C).

Step 8

Determine the critical logarithmic spiral (second successive approximation) for a homogeneous material for which c = 0.437 psi. and ϕ = 30 deg. 26 min., by the trial and error method outlined in Appendix A. The ultimate strength q for this homogeneous material as calculated from this second critical spiral = 34.04 psi. (Table 4).

Step 9

Calculate over-all average values for c and ϕ as given by this second critical spiral, using the procedure described in Steps 4, 5, and 6. These over-all average values are found to be c = 0.739 psi. and ϕ = 30 deg. 44 min. These values are used for the third successive critical spiral.

Step 10

Determine the critical logarithmic spiral (third successive approximation) for a homogeneous material for which c = 0.739 psi. and ϕ = 30 deg. 44 min., by the trial-and-error method outlined in Appendix A. The ultimate strength q for this homogeneous material as calculated from this third critical spiral = 45.7 psi. (Table 4).

Step 11

Repeat for as many further successive approximations as may be required for the accuracy needed; that is, until the percent difference in ultimate strength values between two successive approximations is as small as desired.

From Table 4, it will be observed that the ultimate strength given by the fifth critical spiral (fifth successive approximation) is only 1.4 percent higher than that found for the fourth critical spiral. The fifth, and probably the fourth, and even the third critical spiral, therefore, may in this case provide an ultimate strength value of sufficient accuracy for practical design.

Figure C demonstrates that the critical spirals given by each successive approximation in the above steps lie alternately on either side and successively closer to the ultimate critical spiral that would result from many successive approximations.

Step 12

Determine the value for z, representing the deepest penetration of any logarithmic spiral below the ground surface, by the procedure illustrated in Step 12, Appendix A. The value of z for the fifth critical spiral of Table 4 is found to be 15.2 in.